PHYSICAL REVIEW D **112,** 112010 (2025)

Cross section measurement of $e^+e^- \to f_1(1285)\pi^+\pi^-$ at center-of-mass energies between 3.808 and 4.951 GeV

M. Ablikim *et al.*[*]
(BESIII Collaboration)

(Received 27 January 2025; accepted 7 November 2025; published 15 December 2025)

Using data samples collected by the BESIII detector located at the Beijing Electron Positron Collider, the cross sections of the process $e^+e^- \to f_1(1285)\pi^+\pi^-$ are measured at 45 center-of-mass energies from 3.808 to 4.951 GeV. An investigation on the energy-dependent cross section is performed, and no significant structure is observed.

DOI: 10.1103/567d-cv9k

I. INTRODUCTION

In QCD, spectroscopy of hadrons is key toward understanding strong interactions in the nonperturbative regime, and in particular the study of resonance decays into nontrivial exclusive final states is a way to probe the structure of bound states and their interaction properties. New opportunities are offered by unexpected resonances discovered in the charmonium energy region, where the Y resonances with $J^{PC} = 1^{--}$ can be produced directly in e^+e^- annihilation.

Multiple theoretical approaches have been proposed to describe the Y exotic particles, e.g., as tetraquarks, hadronic molecules, hybrid states, or hadrocharmonia [1–4]. Their compatibility with experimental data has recently been reviewed in detail in Ref. [2]. Currently all of the observed decay modes of the Y are associated with the charm sector, and no light hadron decay modes have been found yet [5]. For example, the BESIII experiment has performed series studies on the exotic states decaying into light hadrons, including $e^+e^- \to K_S^0 K^\pm \pi^\mp \pi^0(\eta)$ [6], $K_S^0 K^\pm \pi^\mp$ [7], $p\bar{n}K_S^0 K^- +$ c.c. [8], $\phi\phi\phi$, $\phi\phi\omega$ [9], $p\bar{p}\pi^0$ [10], $p\bar{p}\eta(\omega)$ [11], $2(p\bar{p})$ [12], $\omega\pi^+\pi^-$ [13], and $\omega\pi^0(\eta)$ [14].

Studying decay modes of Y states to light hadrons is expected to provide information that allows one to distinguish between different theoretical models and to understand strong interaction effects in this energy region. The continued search for light hadron decays helps further to understand the nature of exotic states and charmonium resonances. More explorations of light hadronic final states are desirable to probe the nature of charmoniumlike exotic candidates [15,16]. In particular the hybrid model predicts a sizable coupling between the $Y(4260)$ and charmless decays [16]. Searches for new decay modes of the $Y(4260)$ may provide information that can shed light on its nature.

The process $e^+e^- \to f_1(1285)\pi^+\pi^-$ has been studied only at the *BABAR* experiment, from threshold up to 4.550 GeV [17,18]. It may be used to investigate the decay mode of exotic and charmonium states. In addition, the process $e^+e^- \to f_1(1285)\pi^+\pi^-$ is sensitive to the transition form factors of the axial-vector current [19,20], which is crucial to the hadronic light-by-light scattering in the muon anomalous magnetic moment (α_μ) calculation [19,21,22]. A more precise measurement of this process possibly provides a better input to extracting the transition form factors [19].

In this work, we report the measurement of the process $e^+e^- \to f_1(1285)\pi^+\pi^-$, with $f_1(1285) \to \pi^+\pi^-\eta$ and $\eta \to \gamma\gamma$, based on data collected at the BESIII experiment at 45 center-of-mass energies ($\sqrt{s}$) ranging from 3.808 to 4.951 GeV, with an integrated luminosity of 22.2 fb^{-1} [23–25].

II. BESIII DETECTOR AND MONTE CARLO SIMULATION

The BESIII detector [26] records symmetric e^+e^- collisions provided by the BEPCII storage ring [27] in the center-of-mass energy range from 1.84 to 4.95 GeV, with a peak luminosity of 1.1×10^{33} cm^{-2} s^{-1} achieved at $\sqrt{s} = 3.77$ GeV. BESIII has collected large data samples in this energy region [28,29]. The cylindrical core of the BESIII detector covers 93% of the full solid angle and consists of a helium-based multilayer drift chamber (MDC), a plastic scintillator time-of-flight system (TOF), and a CsI(Tl) electromagnetic calorimeter (EMC), all enclosed in a superconducting solenoidal magnet providing a 1.0 T magnetic field. The solenoid is supported by an octagonal flux-return yoke with resistive plate counter muon identification modules interleaved with steel.

---

[*] Full author list given at the end of the article.

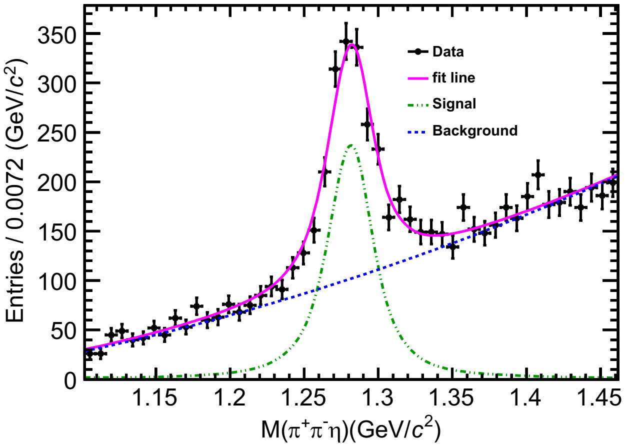

FIG. 1. The $M(\pi^+\pi^-\eta)$ distribution for all four combinations within each event at $\sqrt{s} = 4.178$ GeV. The black dots with error bars are data. The magenta solid line represents the fit result for signal extraction, the green dash-dotted line represents the $f_1(1285)$ shape, and the blue dashed line indicates the background shape.

The charged-particle momentum resolution at 1 GeV/c is 0.5%, and the dE/dx resolution is 6% for electrons from Bhabha scattering. The EMC measures photon energies with a resolution of 2.5% (5%) at 1 GeV in the barrel (end cap) region. The time resolution in the TOF barrel region is 68 ps, while that in the end cap region is 110 ps. The end cap TOF system was upgraded in 2015 using multigap resistive plate chamber technology, providing a time resolution of 60 ps [30]. This improvement affects data at 30 of the 45 center-of-mass energy points.

Simulated data samples produced with a Geant4-based [31] Monte Carlo (MC) package, which includes the geometric description of the BESIII detector and the detector response, are used to determine detection efficiencies and to estimate backgrounds. The simulation models the beam energy spread and initial state radiation (ISR) in the e^+e^- annihilations with the generator KKMC [32]. Signal MC samples for the process $e^+e^- \to f_1(1285)\pi^+\pi^-$ with the subsequent decays $f_1(1285) \to \pi^+\pi^-\eta$ and $\eta \to \gamma\gamma$ are generated uniformly in phase space. The inclusive MC sample includes the production of open charm processes, the ISR production of vector charmonium (like) states, and the continuum processes incorporated in KKMC [32]. All particle decays are modeled with EVTGEN [33] using branching fractions either taken from the Particle Data Group (PDG) [5], when available, or otherwise estimated with LUNDCHARM [34]. Final state radiation from charged final state particles is incorporated using the PHOTOS package [35].

III. EVENT SELECTION AND BACKGROUND ANALYSIS

The process $e^+e^- \to f_1(1285)\pi^+\pi^-$ is reconstructed with $f_1(1285) \to \pi^+\pi^-\eta$ and $\eta \to \gamma\gamma$. Therefore, the final state particles consist of $2(\pi^+\pi^-)$ and 2γ. Charged tracks detected in the MDC are required to be within a polar angle (θ) range of $|\cos\theta| < 0.93$, where θ is defined with respect to the z axis, which is the symmetry axis of the MDC. The distance of closest approach to the interaction point (IP) must be less than 10 cm along the z axis and less than 1 cm in the transverse plane. Exactly four charged tracks with a net charge equal to zero are required. Particle identification (PID) combines information from the energy loss in the MDC and the flight time in the TOF to calculate the probabilities for the π, K, and p hypotheses. Each track is then assigned a particle type corresponding to the hypothesis with the highest probability. Events with four pion candidates are kept for further analysis.

Photon candidates are identified using isolated showers in the EMC. The deposited energy of each shower must be more than 25 MeV in the barrel region ($|\cos\theta| < 0.80$) and more than 50 MeV in the end cap region ($0.86 < |\cos\theta| < 0.92$). To exclude showers that originate from charged tracks, the angle subtended by the EMC shower and the position of the closest charged track at the EMC must be greater than 10° as measured from the IP. To suppress electronic noise and showers unrelated to the event, the difference between the EMC time and the event start time is required to be within [0, 700] ns. Events containing at least two photon candidates are then retained for further analysis. In order to further suppress backgrounds and improve the momentum resolution, a four-constraint kinematic fit is applied that enforces energy-momentum conservation for the $\pi^+\pi^-\pi^+\pi^-\gamma\gamma$ final state. Events are accepted if the fit satisfies $\chi^2 < 100$. If there are more than two photon candidates in addition to the four charged tracks in the event, the combination with the smallest χ^2 is retained. The selection efficiency of the condition $\chi^2 < 100$ for all energy points exceeds 95%.

The η candidate is reconstructed by two photons with $|M(\gamma\gamma) - M(\eta)| < 25$ MeV/c^2, where $M(\gamma\gamma)$ is the invariant mass reconstructed from the two photons and $M(\eta)$ is the known η mass [5].

The invariant mass of $M(\pi^+\pi^-\eta)$ for all four combinations within each event is illustrated in Fig. 1, as an example, using the center-of-mass energy at $\sqrt{s} = 4.178$ GeV that gives the highest statistics among the studied points. A clear $f_1(1285)$ signal is observed. Background contributions are studied through an analysis of the inclusive MC sample with an event-type analysis tool TopoAna [36], indicating that the primary background originates from the continuum process $e^+e^- \to \pi^+\pi^-\pi^+\pi^-\eta$.

IV. CROSS SECTION

The Born cross section at each center-of-mass energy is determined by

$$\sigma_{\mathrm{B}} = \frac{N_{\mathrm{sig}}}{\epsilon \cdot (1+\delta_v) \cdot (1+\delta_\gamma) \cdot \mathcal{B} \cdot \mathcal{L}}, \qquad (1)$$

where $1+\delta_v = \frac{1}{|1-\Pi|^2}$ and $1+\delta_\gamma$ account for the vacuum polarization (VP) and ISR corrections, respectively, and are calculated based on theory [37,38], with numerical values obtained by Monte Carlo integration. The product branching fraction $\mathcal{B} = \mathcal{B}_{f_1(1285)}\mathcal{B}_\eta = 13.8\%$ corresponds to the decay chain $f_1(1285) \to \pi^+\pi^-\eta$ and $\eta \to \gamma\gamma$. The numerator N_{sig} is the signal yield extracted from the fit to $M(\pi^+\pi^-\eta)$ distribution, $\mathcal{L}$ is the integrated luminosity [39–41], and ϵ is the signal detection efficiency. The dressed cross section is obtained by

$$\sigma_{\mathrm{d}} = \sigma_{\mathrm{B}} \cdot (1+\delta_v), \qquad (2)$$

which incorporates the vacuum polarization correction.

The signal yield is obtained through an unbinned maximum likelihood fit to the $M(\pi^+\pi^-\eta)$ distribution. The signal shape is modeled by the MC shape convolved with a Gaussian function to compensate the detector resolution. The MC shape is obtained by matching the reconstructed pions to the truth level ones decayed from $f_1(1285)$ to eliminate effects from incorrect combinations. The background shape is described by a second-order polynomial function. An example of the fit at $\sqrt{s} = 4.178$ GeV is shown in Fig. 1. To prevent distortions from low statistics at other center-of-mass energies, the parameters of the convolved Gaussian function are fixed to the values obtained at $\sqrt{s} = 4.178$ GeV, with a mean $\mu = 0.11$ MeV$/c^2$ and width $\sigma = 0.14$ MeV.

The signal efficiency is obtained from the signal MC sample for $e^+e^- \to f_1(1285)\pi^+\pi^-$, with $f_1(1285) \to \pi^+\pi^-\eta$ and $\eta \to \gamma\gamma$. To reduce discrepancies between data and signal MC, a weighting method is applied to the two-dimensional distributions of $M_{col}(f_1(1285)\pi^+)$ versus $M_{col}(\pi^+\pi^-)$ and $M_{f_1}(\eta\pi^+)$ versus $M_{f_1}(\pi^+\pi^-)$, where pions in M_{col} and M_{f_1} are produced directly in the e^+e^- collisions and from $f_1(1285)$ decay, respectively. These pairs of invariant masses are used to correct the phase space modeling of $f_1(1285)$ production and decay. The $f_1(1285)$ candidates are selected as the $\pi^+\pi^-\eta$ combination with invariant mass closest to the value of $M_{f_1(1285)}$ among the four combinations in an event in the data samples. $M_{f_1(1285)}$ represents the known $f_1(1285)$ mass [5]. Figure 2 shows the comparison on $M(\pi^+\pi^-)$ from e^+e^- collision between data and the weighted signal MC at $\sqrt{s} = 4.178$ GeV.

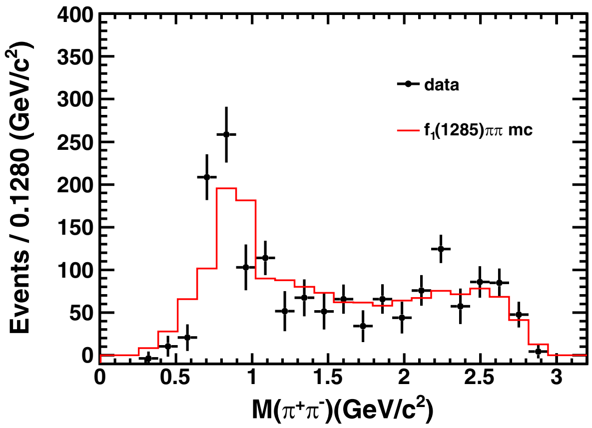

FIG. 2. The distribution of $M(\pi^+\pi^-)$ from e^+e^- collision at $\sqrt{s} = 4.178$ GeV. The black dots with error bars are data; the histogram shows the weighted distribution from signal MC sample.

The correction factors $1+\delta_\gamma$ and ϵ, which depend on the energy-dependent cross section [38], are obtained using an iterative method [42,43]. Both the Born and dressed cross sections follow the trend described by Eq. (3), as discussed in Sec. VI. The iterative process begins with fits to the energy-dependent Born cross section, starting at 3.7 GeV, below the lowest center-of-mass energy in this study. The ϵ and $(1+\delta_\gamma)(1+\delta_v)$ are calculated from the fit curve at each center-of-mass energy and used as input for the next iteration, repeating until the Born cross section converges.

The results of cross sections at each center-of-mass energy are presented in Table I, which includes both statistical and systematic uncertainties for the dressed cross sections (σ_{d}). The statistical uncertainty is originated from the extraction of N_{sig} and given by the fit to $M(\pi^+\pi^-\eta)$ directly. Detailed investigations of the systematic uncertainties are discussed in Sec. V.

V. SYSTEMATIC UNCERTAINTIES

The systematic uncertainties are estimated at each center-of-mass energy. Multiple sources of systematic uncertainties are taken into account in the measurement of the Born cross section for the $e^+e^- \to f_1(1285)\pi^+\pi^-$ process. These include the uncertainties from integrated luminosity measurement, quoted branching fractions, tracking and PID, photon reconstruction, signal yield estimation, kinematic fit, ISR and VP correction factors, as well as uncertainties in signal efficiency associated to weighting method.

The integrated luminosity is determined using large angle Bhabha events, with an uncertainty of 1% [23–25]. The systematic uncertainties of the branching fractions are quoted from the PDG [5], with values of 42.9% and 0.5% for $f_1(1285) \to \eta\pi^+\pi^-$ and $\eta \to \gamma\gamma$, respectively. The systematic uncertainty of the tracking and PID efficiencies are both measured as 1% per track by using control samples $J/\psi \to K_S^0 K^\pm \pi^\mp$, $J/\psi \to p\bar{p}\pi^+\pi^-$, and $J/\psi \to \pi^+\pi^-\pi^0$ [10,44–48]. A systematic uncertainty of 0.2% is assigned to the single-photon reconstruction efficiency using a $J/\psi \to \gamma\mu^+\mu^-$ control sample. Conservatively considering 100% correlation among tracks

TABLE I. Dressed cross sections of the process $e^+e^- \to f_1(1285)\pi^+\pi^-$. $\mathcal{L}$ is the integral luminosity of the data sample at each center-of-mass energy, $N_{\rm sig}$ is the number of signal events, $1+\delta_\gamma$ and $1+\delta_v$ are the converged radiation and vacuum polarization correction factor, respectively, ϵ is the signal efficiency with the weighting method, and $\sigma_{\rm d}$ is the dressed cross section. The first uncertainty in the last column is statistical; the second one is systematic, without including the global systematic uncertainty of 43.3%. A detailed discussion of all systematic uncertainties is provided in Sec. V.

$\sqrt{s}$ (GeV)	$\mathcal{L}$ (pb^{-1})	$N_{\rm sig}$	$1+\delta_\gamma$	$1+\delta_v$	ϵ (%)	$\sigma_{\rm d}$ (pb)
3.808	50.5	56 ± 12	0.86	1.06	22.9	$41.0 \pm 8.8 \pm 0.5$
3.869	219.2	137 ± 22	0.89	1.05	20.9	$24.3 \pm 3.9 \pm 0.3$
3.896	52.6	42 ± 11	0.90	1.05	21.3	$30.1 \pm 7.9 \pm 0.4$
4.008	482.0	331 ± 31	0.94	1.04	19.9	$26.6 \pm 2.5 \pm 0.3$
4.085	52.9	40 ± 10	0.96	1.05	19.5	$29.3 \pm 7.3 \pm 0.4$
4.129	401.5	195 ± 26	0.98	1.05	19.9	$18.2 \pm 2.4 \pm 0.3$
4.158	408.7	179 ± 25	0.98	1.05	19.8	$16.4 \pm 2.3 \pm 0.2$
4.178	3189.0	1593 ± 69	0.99	1.05	18.1	$20.3 \pm 0.9 \pm 0.4$
4.189	526.7	235 ± 27	0.99	1.06	18.4	$17.8 \pm 2.0 \pm 0.2$
4.199	526.0	268 ± 27	0.99	1.06	18.6	$20.1 \pm 2.0 \pm 0.2$
4.209	517.1	227 ± 27	0.99	1.06	18.2	$17.6 \pm 2.1 \pm 0.3$
4.219	514.6	280 ± 28	1.00	1.06	18.3	$21.7 \pm 2.2 \pm 0.2$
4.226	1100.9	494 ± 40	1.00	1.06	18.5	$17.6 \pm 1.4 \pm 0.2$
4.236	530.3	248 ± 27	1.00	1.06	18.6	$18.3 \pm 2.0 \pm 0.3$
4.242	55.9	36 ± 10	1.00	1.06	18.5	$25.3 \pm 7.0 \pm 0.4$
4.244	538.1	212 ± 26	1.00	1.06	18.5	$15.4 \pm 1.9 \pm 0.3$
4.258	828.4	359 ± 33	1.01	1.05	18.2	$17.2 \pm 1.6 \pm 0.2$
4.267	531.1	259 ± 27	1.01	1.05	18.5	$19.0 \pm 2.0 \pm 0.2$
4.278	175.7	67 ± 15	1.01	1.05	18.3	$15.0 \pm 3.4 \pm 0.2$
4.288	502.4	221 ± 25	1.01	1.05	19.2	$16.5 \pm 1.9 \pm 0.2$
4.308	45.1	23 ± 8	1.02	1.05	17.9	$20.4 \pm 7.1 \pm 0.4$
4.313	501.2	244 ± 26	1.02	1.05	19.1	$18.2 \pm 1.9 \pm 0.2$
4.338	505.0	189 ± 25	1.02	1.05	19.4	$13.7 \pm 1.8 \pm 0.2$
4.358	544.0	204 ± 25	1.03	1.05	17.8	$14.9 \pm 1.8 \pm 0.2$
4.378	522.7	201 ± 25	1.03	1.05	19.1	$14.2 \pm 1.8 \pm 0.1$
4.387	55.6	28 ± 9	1.03	1.05	17.5	$20.2 \pm 6.5 \pm 0.3$
4.397	507.8	198 ± 24	1.03	1.05	19.1	$14.3 \pm 1.7 \pm 0.2$
4.416	1043.9	384 ± 34	1.04	1.05	18.8	$13.7 \pm 1.2 \pm 0.2$
4.437	569.9	173 ± 25	1.04	1.05	18.7	$11.3 \pm 1.6 \pm 0.1$
4.467	111.1	51 ± 12	1.05	1.05	18.6	$17.1 \pm 4.0 \pm 0.2$
4.527	112.1	39 ± 9	1.06	1.05	18.5	$12.9 \pm 3.0 \pm 0.2$
4.575	48.9	3^{+4}_{-3}	1.07	1.05	18.6	$2.2^{+3.0}_{-2.2} \pm 0.0$
4.600	586.9	170 ± 22	1.07	1.05	18.4	$10.6 \pm 1.4 \pm 0.2$
4.612	103.7	17 ± 8	1.08	1.05	17.7	$6.2 \pm 2.9 \pm 0.1$
4.628	521.5	183 ± 22	1.08	1.05	17.4	$13.6 \pm 1.6 \pm 0.1$
4.641	551.7	126 ± 20	1.08	1.05	17.7	$8.7 \pm 1.4 \pm 0.1$
4.661	529.4	141 ± 20	1.09	1.05	17.4	$10.2 \pm 1.4 \pm 0.1$
4.682	1667.4	400 ± 35	1.09	1.05	17.4	$9.2 \pm 0.8 \pm 0.1$
4.699	535.5	113 ± 18	1.09	1.05	17.3	$8.1 \pm 1.3 \pm 0.1$
4.740	163.9	37 ± 10	1.10	1.05	17.4	$8.6 \pm 2.3 \pm 0.1$
4.750	366.6	89 ± 16	1.10	1.05	17.4	$9.2 \pm 1.7 \pm 0.1$
4.781	511.5	100 ± 17	1.11	1.06	17.3	$7.4 \pm 1.3 \pm 0.1$
4.843	525.2	105 ± 18	1.12	1.06	17.1	$7.6 \pm 1.3 \pm 0.1$
4.918	207.8	36 ± 9	1.13	1.06	16.7	$6.7 \pm 1.7 \pm 0.1$
4.951	159.3	6^{+8}_{-7}	1.14	1.06	16.6	$1.4^{+1.9}_{-1.7} \pm 0.0$

(or photons), the total systematic uncertainties come from the tracking efficiencies, PID, and photon reconstruction are 4%, 4%, and 0.4%, respectively.

Three sources of the systematic uncertainties are taken into account for signal yield estimation: signal shape, background shape, and fit range. To mitigate the impact of statistical fluctuation, samples from all center-of-mass energies are combined for the systematic study. The discrepancy in the signal yields obtained by using the Breit-Wigner function convolved with a Gaussian instead of the MC shape convolved with a Gaussian function is attributed to the systematic uncertainty arising from the signal shape description. Similarly, the difference in the signal yields when using a third-order polynomial to describe the background shape, as opposed to the nominal method, is taken as the systematic uncertainty stemming from the background shape description. The systematic uncertainty associated with the fit range is determined by comparing the results obtained when enlarging or shrinking the fit range by 10 MeV/c^2 on both sides, with the largest difference compared to the nominal signal yield being considered as the systematic uncertainty. Systematic uncertainties for signal yield estimation from signal shape, background shape, and fit range are 1.5%, 0.7%, and 0.6%, respectively, for all the center-of-mass energy points.

The systematic uncertainty of the kinematic fit is determined by taking into account the track helix correction parameters in the signal MC sample. The value of π-type track correction parameter is obtained from the control sample $e^+e^- \to \pi^+\pi^- J/\psi$. The difference in efficiency from the nominal result is considered as the systematic uncertainty caused by the kinematic fit [49], which gives the uncertainties ranging from 0.3% to 0.7% at different center-of-mass energies.

The systematic uncertainty associated with ISR and VP corrections, as well as signal efficiency are assessed from two perspectives: the iterative method and the choice of start point for the energy-dependent Born cross section fit. By randomly varying the fit parameters [λ and c in Eq. (3)] of converged energy-dependent Born cross section with respect to their correlation matrix based on Gaussian functions for a sufficient number of times (in this analysis, 1000 times are used), a distribution of the new $\epsilon(1+\delta_\gamma)(1+\delta_v)$ with 1000 entries is obtained. The standard deviations of the Gaussian functions are set to the uncertainties of corresponding parameter. This distribution is then fitted by a Gaussian function. The ratio of the width to the mean of the fitted Gaussian distribution is considered as the systematic uncertainty related to the iterative method. It is estimated as 0.04% for all center-of-mass energies, which is negligible and thus ignored. To determine the systematic uncertainty related to the choice of the starting point in the energy-dependent Born cross section fit, the start point is set to 1.8 GeV, close to the production threshold of the $e^+e^- \to f_1(1285)\pi^+\pi^-$ process. For energies below 3.7 GeV, results from the *BABAR* experiment [17] are utilized. Given that KKMC [32] is originally designed for simulating $c\bar{c}$ processes and may not accurately represent processes below the $c\bar{c}$ threshold, the signal MC samples are generated using the CONEXC generator [38] to address the issue. Differences between the two generators are found to be less than 0.2%, which is considered negligible. The systematic uncertainty from the energy-dependent Born cross section fit range is determined by comparing the $\epsilon(1+\delta_\gamma)(1+\delta_v)$ values obtained from the complete energy-dependent Born cross section fit with the nominal values. It ranges from 0.2% to 1.6% at different center-of-mass energy points.

The systematic uncertainty associated with the signal efficiency, derived from the weighting method, is assessed by varying weights of the two-dimensional histograms according to Gaussian distributions with their standard deviations as the corresponding error in the bin. This process is repeated 1000 times to generate a distribution of efficiencies and fitted by a Gaussian function. The systematic uncertainty is determined by the ratio of the width to mean of the fitted Gaussian function, which gives results ranging from 0.7% to 1.0% in the studied center-of-mass energy region.

The total systematic uncertainty at each center-of-mass energy is calculated by summing the individual contributions in quadrature. The systematic uncertainties originating from integrated luminosity, branching fractions, tracking and PID, photon reconstruction, and signal yields from the fit are defined as global uncertainties, as they hold the same value at each center-of-mass energy and treated as fully correlated. These global uncertainties amount to 43.3% totally. Systematic uncertainties associated to ISR and VP correction factors, signal yields from weight, and kinematic fit are center-of-mass energy dependent. Considering the methods how they were obtained, they are also correlated uncertainties. These systematic uncertainties are then propagated to the dressed cross sections using the relation given by Eq. (2).

VI. THE FIT OF $e^+e^- \to f_1(1285)\pi^+\pi^-$ CROSS SECTION

The dressed cross section of the process $e^+e^- \to f_1(1285)\pi^+\pi^-$ is shown in Fig. 3. No obvious resonance

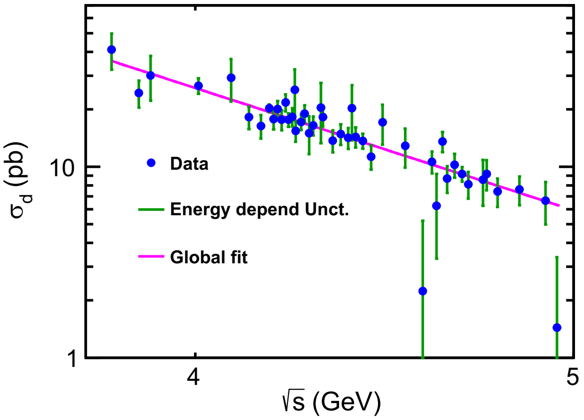

FIG. 3. The energy-dependent dressed cross section of the process $e^+e^- \to f_1(1285)\pi^+\pi^-$. The blue points represent data, with green bars on them showing the total statistical and systematic uncertainties except the global systematic uncertainty of 43.3%. The fit properly accounts for all uncertainties is described by the magenta solid line.

is observed in the energy region from $\sqrt{s} = 3.808$ to 4.951 GeV. The energy-dependent dressed cross section can be described by [10,50]

$$\sigma_{\mathrm{d}} = \left(\frac{c}{\sqrt{s}}\right)^{\lambda}, \tag{3}$$

where c and λ are free parameters to be determined in the fit.

The best fit parameters are determined by minimizing the χ^2 function [51–54]

$$\chi^2 = \sum_{i}^{n}\left(\frac{\sigma_i - f\sigma_i^{\mathrm{fit}}}{\delta_i}\right)^2 + \left(\frac{1-f}{\delta_f}\right)^2, \tag{4}$$

where σ_i and σ_i^{fit} are the measured and fitted dressed cross sections at the ith energy point, respectively. δ_i is the uncorrelated uncertainty, f is the scale factor as a free parameter in the fit, and δ_f is the relative systematic uncertainty of f, determined by the total correlated uncertainties. Systematic uncertainties are treated as correlated, while the statistical ones are uncorrelated. The correlated systematic uncertainties are estimated at each center-of-mass energy, resulting in slight differences at different $\sqrt{s}$. Considering that energy-dependent systematic uncertainties, including sources from ISR and VP correction factors, signal yields from weight, and kinematic fit, are much smaller comparing to the global one. The slight difference of systematic uncertainties at different center-of-mass energies has negligible effects on the fit results. The value at $\sqrt{s} = 4.178$ GeV is taken as δ_f. The fit result is shown in Fig. 3. The p value of the fit is $p = 0.3$. The parameter λ describes the cross section as a function of the center-of-mass energy. The values of $\lambda = 6.61 \pm 0.37 \pm 0.27$ and $c = 6.54 \pm 0.49 \pm 0.55$ are determined from the fit, where the first uncertainties are statistical and the second are systematic. The correlation coefficient between the two parameters is -0.37. Systematic uncertainties for λ and c are derived from the cross section measurement and the fit range of the energy-dependent dressed cross section. By increasing or decreasing the cross section at all center-of-mass energies simultaneously by the systematic uncertainties and comparing to nominal values of the parameters, the larger difference is treated as the systematic uncertainty from cross section measurement. Changing the fit threshold from 3.7 down to 1.8 GeV, the differences comparing to nominal values of the parameters are assigned to the systematic uncertainties due to the choice of the fit range.

To explore the possible resonance contribution, a Breit-Wigner function is added coherently to Eq. (3):

$$\sigma_{\mathrm{d}} = \left[\sqrt{\left(\frac{c}{\sqrt{s}}\right)^{\lambda}} + \frac{\sqrt{12\pi C\Gamma_{ee}\mathcal{B}_{f_1(1285)\pi^+\pi^-}\Gamma}}{s - M^2 + iM\Gamma}e^{i\phi}\right]^2, \tag{5}$$

where Γ_{ee}, $\mathcal{B}_{f_1(1285)\pi^+\pi^-}$, M, Γ, s, ϕ and C are the partial width of the resonance decaying to e^+e^-, the branching fraction of the resonance decaying to $f_1(1285)\pi^+\pi^-$, the mass of the resonance, the width of the resonance, the square of the center-of-mass energy, the relative phase of the resonance compared to the nonresonant process, and a conversion constant equal to 3.894×10^5 nb GeV^2, respectively. In the fit, M and Γ are fixed to the known masses and widths of the resonances $\psi(4040), \psi(4160), \psi(4230), \psi(4360), \psi(4415)$, or $\psi(4660)$ [5], while other parameters including $\Gamma_{ee}\mathcal{B}_{f_1(1285)\pi^+\pi^-}$ and ϕ are left free to vary. The fit is performed individually for each resonance. The number of additional parameters is two, which are $\Gamma_{ee}\mathcal{B}_{f_1(1285)\pi^+\pi^-}$ and ϕ. The significance of all possible resonances is found to be less than 2σ in each case.

VII. SUMMARY

The cross sections of $e^+e^- \to f_1(1285)\pi^+\pi^-$ at center-of-mass energies from 3.808 to 4.951 GeV are reported. The precision is improved by a factor of 2 compared to the previous results [17,18], and the first cross section measurement is provided in a range extending from 4.550 up to 4.951 GeV. From the analysis of energy-dependent dressed cross section as shown in Fig. 3, no significant resonance is observed. The energy-dependent cross section of $e^+e^- \to f_1(1285)\pi^+\pi^-$ can be well described by a power law function. Individual examinations of potential resonance contributions from the charmonium states $\psi(4040)$, $\psi(4160)$, $\psi(4230)$, $\psi(4360)$, $\psi(4415)$, and $\psi(4660)$ indicate that their significance are each below 2 standard deviations. Variation of χ^2 over additional number of freedom (Δn.d.f.) between with out and without resonance considered in the fit is at most $\Delta\chi^2/\Delta\mathrm{n.d.f.} = 1.8/2$.

ACKNOWLEDGMENTS

We are grateful to Dr. Zhilong Han from University of Jinan for his discussions. The BESIII Collaboration thanks the staff of BEPCII and the IHEP computing center for their strong support. This work is supported in part by National Key R&D Program of China under Contracts No. 2020YFA0406300, No. 2020YFA0406400, and No. 2023YFA1606000; National Natural Science Foundation of China (NSFC) under Contracts No. 11635010, No. 11735014, No. 11935015, No. 11935016, No. 11935018, No. 12025502, No. 12035009, No. 12035013, No. 12061131003, No. 12192260, No. 12192261, No. 12192262, No. 12192263, No. 12192264, No. 12192265, No. 12221005, No. 12225509, No. 12235017, and No. 12361141819; the Chinese Academy of Sciences (CAS) Large-Scale Scientific Facility Program; the CAS Center for Excellence in Particle Physics (CCEPP); Joint Large-Scale Scientific Facility Funds of the NSFC and

CAS under Contract No. U1832207; 100 Talents Program of CAS; The Institute of Nuclear and Particle Physics (INPAC) and Shanghai Key Laboratory for Particle Physics and Cosmology; German Research Foundation DFG under Contracts No. 455635585, No. FOR5327, and No. GRK 2149; Istituto Nazionale di Fisica Nucleare, Italy; Ministry of Development of Turkey under Contract No. DPT2006K-120470; National Research Foundation of Korea under Contract No. NRF-2022R1A2C1092335; National Science and Technology fund of Mongolia; National Science Research and Innovation Fund (NSRF) via the Program Management Unit for Human Resources & Institutional Development, Research and Innovation of Thailand under Contract No. B16F640076; Polish National Science Centre under Contract No. 2019/35/O/ST2/02907; The Swedish Research Council; and U.S. Department of Energy under Contract No. DE-FG02-05ER41374. This paper is also supported by the NSFC under Contracts No. 11335008, No. 11605074, No. 12105276, and No. 12205175; Joint Large-Scale Scientific Facility Funds of the NSFC and CAS under Contracts No. U1732263 and No. U2032115; and Natural Science Foundation of Shandong Province under Grant No. ZR2023MA013.

DATA AVAILABILITY

The data that support the findings of this article are not publicly available upon publication because it is not technically feasible and/or the cost of preparing, depositing, and hosting the data would be prohibitive within the terms of this research project. The data are available from the authors upon reasonable request.

[1] N. Brambilla, S. Eidelman, B. K. Heltsley, R. Vogt, G. T. Bodwin, E. Eichten, A. D. Frawley, A. B. Meyer, R. E. Mitchell and V. Papadimitriou *et al.*, Eur. Phys. J. C **71**, 1534 (2011).

[2] N. Brambilla, S. Eidelman, C. Hanhart, A. Nefediev, C. P. Shen, C. E. Thomas, A. Vairo, and C. Z. Yuan, Phys. Rep. **873**, 1 (2020).

[3] F. K. Guo, C. Hanhart, U. G. Meißner, Q. Wang, Q. Zhao, and B. S. Zou, Rev. Mod. Phys. **90**, 015004 (2018); **94**, 029901(E) (2022).

[4] H. X. Chen, W. Chen, X. Liu, and S. L. Zhu, Phys. Rep. **639**, 1 (2016).

[5] S. Navas *et al.* (Particle Data Group), Phys. Rev. D **110**, 030001 (2024).

[6] M. Ablikim *et al.* (BESIII Collaboration), Phys. Rev. D **99**, 012003 (2019).

[7] M. Ablikim *et al.* (BESIII Collaboration), Phys. Rev. D **99**, 072005 (2019).

[8] M. Ablikim *et al.* (BESIII Collaboration), Phys. Rev. D **98**, 032014 (2018).

[9] M. Ablikim *et al.* (BESIII Collaboration), Phys. Lett. B **774**, 78 (2017).

[10] M. Ablikim *et al.* (BESIII Collaboration), Phys. Lett. B **771**, 45 (2017).

[11] M. Ablikim *et al.* (BESIII Collaboration), Phys. Rev. D **104**, 092008 (2021).

[12] M. Ablikim *et al.* (BESIII Collaboration), Phys. Rev. D **103**, 052003 (2021).

[13] M. Ablikim *et al.* (BESIII Collaboration), J. High Energy Phys. 08 (2023) 159.

[14] M. Ablikim *et al.* (BESIII Collaboration), J. High Energy Phys. 07 (2022) 064.

[15] S. Dubynskiy and M. B. Voloshin, Phys. Lett. B **666**, 344 (2008).

[16] F. E. Close and P. R. Page, Phys. Lett. B **628**, 215 (2005).

[17] B. Aubert *et al.* (*BABAR* Collaboration), Phys. Rev. D **76**, 092005 (2007); **77**, 119902(E) (2008).

[18] J. P. Lees *et al.* (*BABAR* Collaboration), Phys. Rev. D **107**, 072001 (2023).

[19] M. Hoferichter, P. Stoffer, and M. Zillinger, Phys. Rev. Lett. **134**, 061902 (2025).

[20] M. Hoferichter, B. Kubis, and M. Zanke, J. High Energy Phys. 08 (2023) 209.

[21] D. P. Aguillard *et al.* (Muon g-2 Collaboration), Phys. Rev. Lett. **131**, 161802 (2023).

[22] D. P. Aguillard *et al.* (Muon g-2 Collaboration), Phys. Rev. D **110**, 032009 (2024).

[23] M. Ablikim *et al.* (BESIII Collaboration), Chin. Phys. C **46**, 113003 (2022).

[24] M. Ablikim *et al.* (BESIII Collaboration), Chin. Phys. C **46**, 113002 (2022).

[25] M. Ablikim *et al.* (BESIII Collaboration), Chin Phys. C **39**, 093001 (2015).

[26] M. Ablikim *et al.* (BESIII Collaboration), Nucl. Instrum. Methods Phys. Res., Sect. A **614**, 345 (2010).

[27] C. Yu *et al.*, *Proceedings of IPAC2016, Busan, Korea* (2016).

[28] M. Ablikim *et al.* (BESII Collaboration), Chin. Phys. C **44**, 040001 (2020).

[29] J. W. Zhang, L. H. Wu, S. S. Sun *et al.*, Radiat. Detect. Technol. Methods **6**, 289 (2022).

[30] X. Li *et al.*, Radiat. Detect. Technol. Methods **1**, 13 (2017); Y. X. Guo *et al.*, Radiat. Detect. Technol. Methods **1**, 15 (2017); P. Cao *et al.*, Nucl. Instrum. Methods Phys. Res., Sect. A **953**, 163053 (2020).

[31] S. Agostinelli *et al.* (GEANT4 Collaboration), Nucl. Instrum. Methods Phys. Res., Sect. A **506**, 250 (2003).

[32] S. Jadach, B. F. L. Ward, and Z. Was, Phys. Rev. D **63**, 113009 (2001); Comput. Phys. Commun. **130**, 260 (2000).

[33] D. J. Lange, Nucl. Instrum. Methods Phys. Res., Sect. A **462**, 152 (2001); R. G. Ping, Chin. Phys. C **32**, 599 (2008).

[34] J. C. Chen, G. S. Huang, X. R. Qi, D. H. Zhang, and Y. S. Zhu, Phys. Rev. D **62**, 034003 (2000); R. L. Yang, R. G. Ping, and H. Chen, Chin. Phys. Lett. **31**, 061301 (2014).

[35] E. Richter-Was, Phys. Lett. B **303**, 163 (1993).

[36] X. Zhou, S. Du, G. Li, and C. Shen, Comput. Phys. Commun. **258**, 107540 (2021).

[37] M. E. Peskin and D. V. Schroeder, *An Introduction to Quantum Field Theory* (Addison-Wesley, Reading, MA, 1995).

[38] R. G. Ping, Chin. Phys. C **38**, 083001 (2014).

[39] G. Goldhaber *et al.*, Phys. Lett. **69B**, 503 (1977).

[40] R. Brandelik *et al.* (DASP Collaboration), Phys. Lett. B **76B**, 361 (1978).

[41] J. Siegrist *et al.*, Phys. Rev. Lett. **36**, 700 (1976).

[42] W. Sun, T. Liu, M. Jing, L. Wang, B. Zhong, and W. Song, Front. Phys. (Beijing) **16**, 64501 (2021).

[43] M. Ablikim *et al.* (BESIII Collaboration), Phys. Rev. D **104**, 092014 (2021).

[44] M. Ablikim *et al.* (BESIII Collaboration), Phys. Rev. Lett. **112**, 022001 (2014).

[45] M. Ablikim *et al.* (BESIII Collaboration), Phys. Rev. D **81**, 052005 (2010).

[46] W. L. Yuan, X. C. Ai, X. B. Ji, S. J. Chen, Y. Zhang, L. H. Wu, L. L. Wang, and Y. Yuan, Chin. Phys. C **40**, 026201 (2016).

[47] M. Ablikim *et al.* (BESIII Collaboration), Phys. Rev. D **86**, 092009 (2012).

[48] M. Ablikim *et al.* (BESIII Collaboration), Phys. Rev. D **83**, 112005 (2011).

[49] M. Ablikim *et al.* (BESIII Collaboration), Phys. Rev. D **87**, 012002 (2013).

[50] M. Ablikim *et al.* (BESIII Collaboration), Phys. Rev. D **108**, 032004 (2023).

[51] X. H. Mo, Chin. Phys. C **30**, 140 (2006).

[52] X. H. Mo and Y. S. Zhu, Chin. Phys. C **27**, 747 (2003).

[53] X. H. Mo and Y. S. Zhu, Chin. Phys. C **27**, 371 (2003).

[54] X. H. Mo, Chin. Phys. C **31**, 745 (2007).

M. Ablikim,[1] M. N. Achasov,[4,c] P. Adlarson,[76] O. Afedulidis,[3] X. C. Ai,[81] R. Aliberti,[35] A. Amoroso,[75a,75c] Q. An,[72,58,a]
Y. Bai,[57] O. Bakina,[36] I. Balossino,[29a] Y. Ban,[46,h] H.-R. Bao,[64] V. Batozskaya,[1,44] K. Begzsuren,[32] N. Berger,[35]
M. Berlowski,[44] M. Bertani,[28a] D. Bettoni,[29a] F. Bianchi,[75a,75c] E. Bianco,[75a,75c] A. Bortone,[75a,75c] I. Boyko,[36] R. A. Briere,[5]
A. Brueggemann,[69] H. Cai,[77] X. Cai,[1,58] A. Calcaterra,[28a] G. F. Cao,[1,64] N. Cao,[1,64] S. A. Cetin,[62a] J. F. Chang,[1,58]
G. R. Che,[43] G. Chelkov,[36,b] C. Chen,[43] C. H. Chen,[9] Chao Chen,[55] G. Chen,[1] H. S. Chen,[1,64] H. Y. Chen,[20] M. L. Chen,[1,58,64]
S. J. Chen,[42] S. L. Chen,[45] S. M. Chen,[61] T. Chen,[1,64] X. R. Chen,[31,64] X. T. Chen,[1,64] Y. B. Chen,[1,58] Y. Q. Chen,[34]
Z. J. Chen,[25,I] Z. Y. Chen,[1,64] S. K. Choi,[10] G. Cibinetto,[29a] F. Cossio,[75c] J. J. Cui,[50] H. L. Dai,[1,58] J. P. Dai,[79] A. Dbeyssi,[18]
R. E. de Boer,[3] D. Dedovich,[36] C. Q. Deng,[73] Z. Y. Deng,[1] A. Denig,[35] I. Denysenko,[36] M. Destefanis,[75a,75c]
F. De Mori,[75a,75c] B. Ding,[67,1] X. X. Ding,[46,h] Y. Ding,[40] Y. Ding,[34] J. Dong,[1,58] L. Y. Dong,[1,64] M. Y. Dong,[1,58,64] X. Dong,[77]
M. C. Du,[1] S. X. Du,[81] Y. Y. Duan,[55] Z. H. Duan,[42] P. Egorov,[36,b] Y. H. Fan,[45] J. Fang,[1,58] J. Fang,[59] S. S. Fang,[1,64]
W. X. Fang,[1] Y. Fang,[1] Y. Q. Fang,[1,58] R. Farinelli,[29a] L. Fava,[75b,75c] F. Feldbauer,[3] G. Felici,[28a] C. Q. Feng,[72,58] J. H. Feng,[59]
Y. T. Feng,[72,58] M. Fritsch,[3] C. D. Fu,[1] J. L. Fu,[64] Y. W. Fu,[1,64] H. Gao,[64] X. B. Gao,[41] Y. N. Gao,[46,h] Yang Gao,[72,58]
S. Garbolino,[75c] I. Garzia,[29a,29b] L. Ge,[81] P. T. Ge,[19] Z. W. Ge,[42] C. Geng,[59] E. M. Gersabeck,[68] A. Gilman,[70] K. Goetzen,[13]
L. Gong,[40] W. X. Gong,[1,58] W. Gradl,[35] S. Gramigna,[29a,29b] M. Greco,[75a,75c] M. H. Gu,[1,58] Y. T. Gu,[15] C. Y. Guan,[1,64]
A. Q. Guo,[31,64] L. B. Guo,[41] M. J. Guo,[50] R. P. Guo,[49] Y. P. Guo,[12,g] A. Guskov,[36,b] J. Gutierrez,[27] K. L. Han,[64] T. T. Han,[1]
F. Hanisch,[3] X. Q. Hao,[19] F. A. Harris,[66] K. K. He,[55] K. L. He,[1,64] F. H. Heinsius,[3] C. H. Heinz,[35] Y. K. Heng,[1,58,64]
C. Herold,[60] T. Holtmann,[3] P. C. Hong,[34] G. Y. Hou,[1,64] X. T. Hou,[1,64] Y. R. Hou,[64] Z. L. Hou,[1] B. Y. Hu,[59] H. M. Hu,[1,64]
J. F. Hu,[56,j] S. L. Hu,[12,g] T. Hu,[1,58,64] Y. Hu,[1] G. S. Huang,[72,58] K. X. Huang,[59] L. Q. Huang,[31,64] X. T. Huang,[50] Y. P. Huang,[1]
Y. S. Huang,[59] T. Hussain,[74] F. Hölzken,[3] N. Hüsken,[35] N. in der Wiesche,[69] J. Jackson,[27] S. Janchiv,[32] J. H. Jeong,[10] Q. Ji,[1]
Q. P. Ji,[19] W. Ji,[1,64] X. B. Ji,[1,64] X. L. Ji,[1,58] Y. Y. Ji,[50] X. Q. Jia,[50] Z. K. Jia,[72,58] D. Jiang,[1,64] H. B. Jiang,[77] P. C. Jiang,[46,h]
S. S. Jiang,[39] T. J. Jiang,[16] X. S. Jiang,[1,58,64] Y. Jiang,[64] J. B. Jiao,[50] J. K. Jiao,[34] Z. Jiao,[23] S. Jin,[42] Y. Jin,[67] M. Q. Jing,[1,64]
X. M. Jing,[64] T. Johansson,[76] S. Kabana,[33] N. Kalantar-Nayestanaki,[65] X. L. Kang,[9] X. S. Kang,[40] M. Kavatsyuk,[65]
B. C. Ke,[81] V. Khachatryan,[27] A. Khoukaz,[69] R. Kiuchi,[1] O. B. Kolcu,[62a] B. Kopf,[3] M. Kuessner,[3] X. Kui,[1,64] N. Kumar,[26]
A. Kupsc,[44,76] W. Kühn,[37] J. J. Lane,[68] L. Lavezzi,[75a,75c] T. T. Lei,[72,58] Z. H. Lei,[72,58] M. Lellmann,[35] T. Lenz,[35] C. Li,[47]
C. Li,[43] C. H. Li,[39] Cheng Li,[72,58] D. M. Li,[81] F. Li,[1,58] G. Li,[1] H. B. Li,[1,64] H. J. Li,[19] H. N. Li,[56,j] Hui Li,[43] J. R. Li,[61]
J. S. Li,[59] K. Li,[1] L. J. Li,[1,64] L. K. Li,[1] Lei Li,[48] M. H. Li,[43] P. R. Li,[38,k,l] Q. M. Li,[1,64] Q. X. Li,[50] R. Li,[17,31] S. X. Li,[12] T. Li,[50]
W. D. Li,[1,64] W. G. Li,[1,a] X. Li,[1,64] X. H. Li,[72,58] X. L. Li,[50] X. Y. Li,[1,64] X. Z. Li,[59] Y. G. Li,[46,h] Z. J. Li,[59] Z. Y. Li,[79]
C. Liang,[42] H. Liang,[72,58] Hao Liang,[1,64] Y. F. Liang,[54] Y. T. Liang,[31,64] G. R. Liao,[14] Y. P. Liao,[1,64] J. Libby,[26] A. Limphirat,[60]
C. C. Lin,[55] D. X. Lin,[31,64] T. Lin,[1] B. J. Liu,[1] B. X. Liu,[77] C. Liu,[34] C. X. Liu,[1] D. Liu,[72,18] F. Liu,[1] F. H. Liu,[53] Feng Liu,[6]
G. M. Liu,[56,j] H. Liu,[38,k,l] H. B. Liu,[15] H. H. Liu,[1] H. M. Liu,[1,64] Huihui Liu,[21] J. B. Liu,[72,58] J. Y. Liu,[1,64] K. Liu,[38,k,l]

K. Y. Liu,[40] Ke Liu,[22] L. Liu,[72,58] L. C. Liu,[43] Lu Liu,[43] M. H. Liu,[12,g] P. L. Liu,[1] Q. Liu,[64] S. B. Liu,[72,58] T. Liu,[12,g]
W. K. Liu,[43] W. M. Liu,[72,58] X. Liu,[38,k,l] X. Liu,[39] Y. Liu,[38,k,l] Y. Liu,[81] Y. B. Liu,[43] Z. A. Liu,[1,58,64] Z. D. Liu,[9] Z. Q. Liu,[50]
X. C. Lou,[1,58,64] F. X. Lu,[59] H. J. Lu,[23] J. G. Lu,[1,58] X. L. Lu,[1] Y. Lu,[7] Y. P. Lu,[1,58] Z. H. Lu,[1,64] C. L. Luo,[41] J. R. Luo,[59]
M. X. Luo,[80] T. Luo,[12,g] X. L. Luo,[1,58] X. R. Lyu,[64] Y. F. Lyu,[43] F. C. Ma,[40] H. Ma,[79] H. L. Ma,[1] J. L. Ma,[1,64] L. L. Ma,[50]
L. R. Ma,[67] M. M. Ma,[1,64] Q. M. Ma,[1] R. Q. Ma,[1,64] T. Ma,[72,58] X. T. Ma,[1,64] X. Y. Ma,[1,58] Y. Ma,[46,h] Y. M. Ma,[31]
F. E. Maas,[18] M. Maggiora,[75a,75c] S. Malde,[70] Y. J. Mao,[46,h] Z. P. Mao,[1] S. Marcello,[75a,75c] Z. X. Meng,[67]
J. G. Messchendorp,[13,65] G. Mezzadri,[29a] H. Miao,[1,64] T. J. Min,[42] R. E. Mitchell,[27] X. H. Mo,[1,58,64] B. Moses,[27]
N. Yu. Muchnoi,[4,c] J. Muskalla,[35] Y. Nefedov,[36] F. Nerling,[18,e] L. S. Nie,[20] I. B. Nikolaev,[4,c] Z. Ning,[1,58] S. Nisar,[11,m]
Q. L. Niu,[38,k,l] W. D. Niu,[55] Y. Niu,[50] S. L. Olsen,[64] Q. Ouyang,[1,58,64] S. Pacetti,[28b,28c] X. Pan,[55] Y. Pan,[57] A. Pathak,[34]
Y. P. Pei,[72,58] M. Pelizaeus,[3] H. P. Peng,[72,58] Y. Y. Peng,[38,k,l] K. Peters,[13,e] J. L. Ping,[41] R. G. Ping,[1,64] S. Plura,[35] V. Prasad,[33]
F. Z. Qi,[1] H. Qi,[72,58] H. R. Qi,[61] M. Qi,[42] T. Y. Qi,[12,g] S. Qian,[1,58] W. B. Qian,[64] C. F. Qiao,[64] X. K. Qiao,[81] J. J. Qin,[73]
L. Q. Qin,[14] L. Y. Qin,[72,58] X. P. Qin,[12,g] X. S. Qin,[50] Z. H. Qin,[1,58] J. F. Qiu,[1] Z. H. Qu,[73] C. F. Redmer,[35] K. J. Ren,[39]
A. Rivetti,[75c] M. Rolo,[75c] G. Rong,[1,64] Ch. Rosner,[18] S. N. Ruan,[43] N. Salone,[44] A. Sarantsev,[36,d] Y. Schelhaas,[35]
K. Schoenning,[76] M. Scodeggio,[29a] K. Y. Shan,[12,g] W. Shan,[24] X. Y. Shan,[72,58] Z. J. Shang,[38,k,l] J. F. Shangguan,[16]
L. G. Shao,[1,64] M. Shao,[72,58] C. P. Shen,[12,g] H. F. Shen,[1,8] W. H. Shen,[64] X. Y. Shen,[1,64] B. A. Shi,[64] H. Shi,[72,58] H. C. Shi,[72,58]
J. L. Shi,[12,g] J. Y. Shi,[1] Q. Q. Shi,[55] S. Y. Shi,[73] X. Shi,[1,58] J. J. Song,[19] T. Z. Song,[59] W. M. Song,[34,1] Y. J. Song,[12,g]
Y. X. Song,[46,h,n] S. Sosio,[75a,75c] S. Spataro,[75a,75c] F. Stieler,[35] Y. J. Su,[64] G. B. Sun,[77] G. X. Sun,[1] H. Sun,[64] H. K. Sun,[1]
J. F. Sun,[19] K. Sun,[61] L. Sun,[77] S. S. Sun,[1,64] T. Sun,[51,f] W. Y. Sun,[34] Y. Sun,[9] Y. J. Sun,[72,58] Y. Z. Sun,[1] Z. Q. Sun,[1,64]
Z. T. Sun,[50] C. J. Tang,[54] G. Y. Tang,[1] J. Tang,[59] M. Tang,[72,58] Y. A. Tang,[77] L. Y. Tao,[73] Q. T. Tao,[25,i] M. Tat,[70]
J. X. Teng,[72,58] V. Thoren,[76] W. H. Tian,[59] Y. Tian,[31,64] Z. F. Tian,[77] I. Uman,[62b] Y. Wan,[55] S. J. Wang,[50] B. Wang,[1]
B. L. Wang,[64] Bo Wang,[72,58] D. Y. Wang,[46,h] F. Wang,[73] H. J. Wang,[38,k,l] J. J. Wang,[77] J. P. Wang,[50] K. Wang,[1,58]
L. L. Wang,[1] M. Wang,[50] N. Y. Wang,[64] S. Wang,[12,g] S. Wang,[38,k,l] T. Wang,[12,g] T. J. Wang,[43] W. Wang,[59] Wei Wang,[73]
W. P. Wang,[72,58] W. P. Wang,[35,72,o] X. Wang,[46,h] X. F. Wang,[38,k,l] X. J. Wang,[39] X. L. Wang,[12,g] X. N. Wang,[1] Y. Wang,[61]
Y. D. Wang,[45] Y. F. Wang,[1,58,64] Y. L. Wang,[19] Y. N. Wang,[45] Y. Q. Wang,[1] Yaqian Wang,[17] Yi Wang,[61] Z. Wang,[1,58]
Z. L. Wang,[73] Z. Y. Wang,[1,64] Ziyi Wang,[64] D. H. Wei,[14] F. Weidner,[69] S. P. Wen,[1] Y. R. Wen,[39] U. Wiedner,[3] G. Wilkinson,[70]
M. Wolke,[76] L. Wollenberg,[3] C. Wu,[39] J. F. Wu,[1,8] L. H. Wu,[1] L. J. Wu,[1,64] X. Wu,[12,g] X. H. Wu,[34] Y. Wu,[72,58] Y. H. Wu,[55]
Y. J. Wu,[31] Z. Wu,[1,58] L. Xia,[72,58] X. M. Xian,[39] B. H. Xiang,[1,64] T. Xiang,[46,g] D. Xiao,[38,k,l] G. Y. Xiao,[42] S. Y. Xiao,[1]
Y. L. Xiao,[12,g] Z. J. Xiao,[41] C. Xie,[42] X. H. Xie,[46,h] Y. Xie,[50] Y. G. Xie,[1,58] Y. H. Xie,[6] Z. P. Xie,[72,58] T. Y. Xing,[1,64]
C. F. Xu,[1,64] C. J. Xu,[59] G. F. Xu,[1] H. Y. Xu,[67,2] M. Xu,[72,58] Q. J. Xu,[16] Q. N. Xu,[30] W. Xu,[1] W. L. Xu,[67] X. P. Xu,[55]
Y. C. Xu,[78] Z. S. Xu,[64] F. Yan,[12,g] L. Yan,[12,g] W. B. Yan,[72,58] W. C. Yan,[81] X. Q. Yan,[1,64] H. J. Yang,[51,f] H. L. Yang,[34]
H. X. Yang,[1] T. Yang,[1] Y. Yang,[12,g] Y. F. Yang,[1,64] Y. F. Yang,[43] Y. X. Yang,[1,64] Z. W. Yang,[38,k,l] Z. P. Yao,[50] M. Ye,[1,58]
M. H. Ye,[8] J. H. Yin,[1] Junhao Yin,[43] Z. Y. You,[59] B. X. Yu,[1,58,64] C. X. Yu,[43] G. Yu,[1,64] J. S. Yu,[25,i] T. Yu,[73] X. D. Yu,[46,h]
Y. C. Yu,[81] C. Z. Yuan,[1,64] J. Yuan,[34] J. Yuan,[45] L. Yuan,[2] S. C. Yuan,[1,64] Y. Yuan,[1,64] Z. Y. Yuan,[59] C. X. Yue,[39] A. A. Zafar,[74]
F. R. Zeng,[50] S. H. Zeng,[63] X. Zeng,[12,g] Y. Zeng,[25,i] Yujie Zeng,[59] Y. J. Zeng,[1,64] X. Y. Zhai,[34] Y. C. Zhai,[50] Y. H. Zhan,[59]
A. Q. Zhang,[1,64] B. L. Zhang,[1,64] B. X. Zhang,[1] D. H. Zhang,[43] G. Y. Zhang,[19] H. Zhang,[72,58] H. Zhang,[81] H. C. Zhang,[1,58,64]
H. H. Zhang,[59] H. H. Zhang,[34] H. Q. Zhang,[1,58,64] H. R. Zhang,[72,58] H. Y. Zhang,[1,58] Jin Zhang,[81] J. Zhang,[59] J. J. Zhang,[52]
J. L. Zhang,[20] J. Q. Zhang,[41] J. S. Zhang,[12,g] J. W. Zhang,[1,58,64] J. X. Zhang,[38,k,l] J. Y. Zhang,[1] J. Z. Zhang,[1,64]
Jianyu Zhang,[64] L. M. Zhang,[61] Lei Zhang,[42] P. Zhang,[1,64] Q. Y. Zhang,[34] R. Y. Zhang,[38,k,l] S. H. Zhang,[1,64] Shulei Zhang,[25,i]
X. D. Zhang,[45] X. M. Zhang,[1] X. Y. Zhang,[50] Y. Zhang,[1] Y. Zhang,[73] Y. T. Zhang,[81] Y. H. Zhang,[1,58] Y. M. Zhang,[39]
Yan Zhang,[72,58] Z. D. Zhang,[1] Z. H. Zhang,[1] Z. L. Zhang,[34] Z. Y. Zhang,[77] Z. Y. Zhang,[43] Z. Z. Zhang,[45] G. Zhao,[1]
J. Y. Zhao,[1,64] J. Z. Zhao,[1,58] L. Zhao,[1] Lei Zhao,[72,58] M. G. Zhao,[43] N. Zhao,[79] R. P. Zhao,[64] S. J. Zhao,[81] Y. B. Zhao,[1,58]
Y. X. Zhao,[31,64] Z. G. Zhao,[72,58] A. Zhemchugov,[36,b] B. Zheng,[73] B. M. Zheng,[34] J. P. Zheng,[1,58] W. J. Zheng,[1,64]
Y. H. Zheng,[64] B. Zhong,[41] X. Zhong,[59] H. Zhou,[50] J. Y. Zhou,[34] L. P. Zhou,[1,64] S. Zhou,[6] X. Zhou,[77] X. K. Zhou,[6]
X. R. Zhou,[72,58] X. Y. Zhou,[39] Y. Z. Zhou,[12,g] A. N. Zhu,[64] J. Zhu,[43] K. Zhu,[1] K. J. Zhu,[1,58,64] K. S. Zhu,[12,g] L. Zhu,[34]
L. X. Zhu,[64] S. H. Zhu,[71] T. J. Zhu,[12,g] W. D. Zhu,[41] Y. C. Zhu,[72,58] Z. A. Zhu,[1,64] J. H. Zou,[1] and J. Zu[72,58]

(BESIII Collaboration)

[1]*Institute of High Energy Physics, Beijing 100049, People's Republic of China*
[2]*Beihang University, Beijing 100191, People's Republic of China*
[3]*Bochum Ruhr-University, D-44780 Bochum, Germany*
[4]*Budker Institute of Nuclear Physics SB RAS (BINP), Novosibirsk 630090, Russia*
[5]*Carnegie Mellon University, Pittsburgh, Pennsylvania 15213, USA*
[6]*Central China Normal University, Wuhan 430079, People's Republic of China*
[7]*Central South University, Changsha 410083, People's Republic of China*
[8]*China Center of Advanced Science and Technology, Beijing 100190, People's Republic of China*
[9]*China University of Geosciences, Wuhan 430074, People's Republic of China*
[10]*Chung-Ang University, Seoul, 06974, Republic of Korea*
[11]*COMSATS University Islamabad, Lahore Campus, Defence Road,*
Off Raiwind Road, 54000 Lahore, Pakistan
[12]*Fudan University, Shanghai 200433, People's Republic of China*
[13]*GSI Helmholtzcentre for Heavy Ion Research GmbH, D-64291 Darmstadt, Germany*
[14]*Guangxi Normal University, Guilin 541004, People's Republic of China*
[15]*Guangxi University, Nanning 530004, People's Republic of China*
[16]*Hangzhou Normal University, Hangzhou 310036, People's Republic of China*
[17]*Hebei University, Baoding 071002, People's Republic of China*
[18]*Helmholtz Institute Mainz, Staudinger Weg 18, D-55099 Mainz, Germany*
[19]*Henan Normal University, Xinxiang 453007, People's Republic of China*
[20]*Henan University, Kaifeng 475004, People's Republic of China*
[21]*Henan University of Science and Technology, Luoyang 471003, People's Republic of China*
[22]*Henan University of Technology, Zhengzhou 450001, People's Republic of China*
[23]*Huangshan College, Huangshan 245000, People's Republic of China*
[24]*Hunan Normal University, Changsha 410081, People's Republic of China*
[25]*Hunan University, Changsha 410082, People's Republic of China*
[26]*Indian Institute of Technology Madras, Chennai 600036, India*
[27]*Indiana University, Bloomington, Indiana 47405, USA*
[28a]*INFN Laboratori Nazionali di Frascati, INFN Laboratori Nazionali di Frascati, I-00044, Frascati, Italy*
[28b]*INFN Sezione di Perugia, I-06100, Perugia, Italy*
[28c]*University of Perugia, I-06100, Perugia, Italy*
[29a]*INFN Sezione di Ferrara, INFN Sezione di Ferrara, I-44122, Ferrara, Italy*
[29b]*University of Ferrara, I-44122, Ferrara, Italy*
[30]*Inner Mongolia University, Hohhot 010021, People's Republic of China*
[31]*Institute of Modern Physics, Lanzhou 730000, People's Republic of China*
[32]*Institute of Physics and Technology, Peace Avenue 54B, Ulaanbaatar 13330, Mongolia*
[33]*Instituto de Alta Investigación, Universidad de Tarapacá, Casilla 7D, Arica 1000000, Chile*
[34]*Jilin University, Changchun 130012, People's Republic of China*
[35]*Johannes Gutenberg University of Mainz, Johann-Joachim-Becher-Weg 45, D-55099 Mainz, Germany*
[36]*Joint Institute for Nuclear Research, 141980 Dubna, Moscow region, Russia*
[37]*Justus-Liebig-Universitaet Giessen, II. Physikalisches Institut,*
Heinrich-Buff-Ring 16, D-35392 Giessen, Germany
[38]*Lanzhou University, Lanzhou 730000, People's Republic of China*
[39]*Liaoning Normal University, Dalian 116029, People's Republic of China*
[40]*Liaoning University, Shenyang 110036, People's Republic of China*
[41]*Nanjing Normal University, Nanjing 210023, People's Republic of China*
[42]*Nanjing University, Nanjing 210093, People's Republic of China*
[43]*Nankai University, Tianjin 300071, People's Republic of China*
[44]*National Centre for Nuclear Research, Warsaw 02-093, Poland*
[45]*North China Electric Power University, Beijing 102206, People's Republic of China*
[46]*Peking University, Beijing 100871, People's Republic of China*
[47]*Qufu Normal University, Qufu 273165, People's Republic of China*
[48]*Renmin University of China, Beijing 100872, People's Republic of China*
[49]*Shandong Normal University, Jinan 250014, People's Republic of China*
[50]*Shandong University, Jinan 250100, People's Republic of China*
[51]*Shanghai Jiao Tong University, Shanghai 200240, People's Republic of China*
[52]*Shanxi Normal University, Linfen 041004, People's Republic of China*
[53]*Shanxi University, Taiyuan 030006, People's Republic of China*
[54]*Sichuan University, Chengdu 610064, People's Republic of China*
[55]*Soochow University, Suzhou 215006, People's Republic of China*

[56]*South China Normal University, Guangzhou 510006, People's Republic of China*
[57]*Southeast University, Nanjing 211100, People's Republic of China*
[58]*State Key Laboratory of Particle Detection and Electronics, Beijing 100049, Hefei 230026, People's Republic of China*
[59]*Sun Yat-Sen University, Guangzhou 510275, People's Republic of China*
[60]*Suranaree University of Technology, University Avenue 111, Nakhon Ratchasima 30000, Thailand*
[61]*Tsinghua University, Beijing 100084, People's Republic of China*
[62a]*Turkish Accelerator Center Particle Factory Group, Istinye University, 34010, Istanbul, Turkey*
[62b]*Near East University, Nicosia, North Cyprus, 99138, Mersin 10, Turkey*
[63]*University of Bristol, H H Wills Physics Laboratory, Tyndall Avenue, Bristol, BS8 1TL, United Kingdom*
[64]*University of Chinese Academy of Sciences, Beijing 100049, People's Republic of China*
[65]*University of Groningen, NL-9747 AA Groningen, The Netherlands*
[66]*University of Hawaii, Honolulu, Hawaii 96822, USA*
[67]*University of Jinan, Jinan 250022, People's Republic of China*
[68]*University of Manchester, Oxford Road, Manchester, M13 9PL, United Kingdom*
[69]*University of Muenster, Wilhelm-Klemm-Strasse 9, 48149 Muenster, Germany*
[70]*University of Oxford, Keble Road, Oxford OX13RH, United Kingdom*
[71]*University of Science and Technology Liaoning, Anshan 114051, People's Republic of China*
[72]*University of Science and Technology of China, Hefei 230026, People's Republic of China*
[73]*University of South China, Hengyang 421001, People's Republic of China*
[74]*University of the Punjab, Lahore-54590, Pakistan*
[75a]*University of Turin and INFN, University of Turin, I-10125, Turin, Italy*
[75b]*University of Eastern Piedmont, I-15121, Alessandria, Italy*
[75c]*INFN, I-10125, Turin, Italy*
[76]*Uppsala University, Box 516, SE-75120 Uppsala, Sweden*
[77]*Wuhan University, Wuhan 430072, People's Republic of China*
[78]*Yantai University, Yantai 264005, People's Republic of China*
[79]*Yunnan University, Kunming 650500, People's Republic of China*
[80]*Zhejiang University, Hangzhou 310027, People's Republic of China*
[81]*Zhengzhou University, Zhengzhou 450001, People's Republic of China*

[a] Deceased.

[b] Also at the Moscow Institute of Physics and Technology, Moscow 141700, Russia.

[c] Also at the Novosibirsk State University, Novosibirsk, 630090, Russia.

[d] Also at the NRC "Kurchatov Institute," PNPI, 188300, Gatchina, Russia.

[e] Also at Goethe University Frankfurt, 60323 Frankfurt am Main, Germany.

[f] Also at Key Laboratory for Particle Physics, Astrophysics and Cosmology, Ministry of Education; Shanghai Key Laboratory for Particle Physics and Cosmology; Institute of Nuclear and Particle Physics, Shanghai 200240, People's Republic of China.

[g] Also at Key Laboratory of Nuclear Physics and Ion-beam Application (MOE) and Institute of Modern Physics, Fudan University, Shanghai 200443, People's Republic of China.

[h] Also at State Key Laboratory of Nuclear Physics and Technology, Peking University, Beijing 100871, People's Republic of China.

[i] Also at School of Physics and Electronics, Hunan University, Changsha 410082, China.

[j] Also at Guangdong Provincial Key Laboratory of Nuclear Science, Institute of Quantum Matter, South China Normal University, Guangzhou 510006, China.

[k] Also at MOE Frontiers Science Center for Rare Isotopes, Lanzhou University, Lanzhou 730000, People's Republic of China.

[l] Also at Lanzhou Center for Theoretical Physics, Lanzhou University, Lanzhou 730000, People's Republic of China.

[m] Also at the Department of Mathematical Sciences, IBA, Karachi 75270, Pakistan.

[n] Also at Ecole Polytechnique Federale de Lausanne (EPFL), CH-1015 Lausanne, Switzerland.

[o] Also at Helmholtz Institute Mainz, Staudinger Weg 18, D-55099 Mainz, Germany.